Hindawi
International Journal of Mathematics and Mathematical Sciences
Volume 2022, Article ID 5410754, 11 pages
https://doi.org/10.1155/2022/5410754

Research Article

A Fitted Mesh Cubic Spline in Tension Method for Singularly Perturbed Problems with Two Parameters

Tariku Birabasa Mekonnen [1] **and Gemechis File Duressa** [2]

[1]*Department of Mathematics, Wollega University, Nekemte, Ethiopia*
[2]*Department of Mathematics, Jimma University, Jimma, Ethiopia*

Correspondence should be addressed to Tariku Birabasa Mekonnen; seenaa29@gmail.com

Received 7 December 2021; Accepted 7 January 2022; Published 15 February 2022

Academic Editor: Niansheng Tang

A numerical treatment via a difference scheme constructed by the Crank–Nicolson scheme for the time derivative and cubic spline in tension for the spatial derivatives on a layer resolving nonuniform Bakhvalov-type mesh for a singularly perturbed unsteady-state initial-boundary-value problem with two small parameters is presented. Error analysis of the constructed scheme is discussed and shown to be parameter-uniformly convergent with second-order convergence. Numerical experimentation is taken to confirm the theoretical findings.

1. Introduction

The following class of unsteady-state singularly perturbed one-dimensional parabolic convection-diffusion problems

$$L_{\varepsilon,\mu}u \coloneqq \frac{\partial u}{\partial t} - \varepsilon\frac{\partial^2 u}{\partial x^2} - \mu a(x,t)\frac{\partial u}{\partial x} + b(x,t)u = f(x,t), \quad (1)$$

on the domain $D = \Omega \times (0,T], \Omega = (0,1)$, together with prescribed initial and boundary conditions of Dirichlet-type,

$$\begin{aligned} u(x,0) &= s(x), x \in \overline{\Omega}, \\ u(0,t) &= 0 = u(1,t), t \in [0,T], \end{aligned} \quad (2)$$

where $0 < \varepsilon \ll 1$ and $0 \le \mu \ll 1$ are two small positive parameters considered. The functions $a(x,t), b(x,t), f(x,t)$, and $s(x)$ are assumed to be sufficiently smooth satisfying $a(x,t) \ge \alpha > 0, b(x,t) \ge \beta > 0, \forall (x,t) \in \overline{D}$. Furthermore, we assume the compatibility condition at the two corner points, i.e., $u(0,0) = s(0), u(1,0) = s(1)$. Within this frame, a unique solution $u(x,t)$ exists for the problem and exhibits a boundary layer on both the left and right lateral boundaries of the spatial domain $\overline{\Omega}$ with significantly different width depending on the relation between μ^2 and ε [1–6].

Singularly perturbed problems (SPPs) widely appear in modeling physical problems such as fluid dynamics, heat and mass transfer in chemical engineering, quantum mechanics [7], elasticity, the theory of plates and shells, oil and gas reservoir simulation, and magnetic-hydrodynamic flow in general [2] and two-parameter singularly perturbed problems (TPSPPs) occur in chemical flow reactor theory [5] as well as in the case of boundary layers controlled by suction (or blowing) of some fluid [8] in particular.

Several articles dealt with the solution of an SPP and showed that it is revealed to have a sudden change in the boundary layer region and behaves normally in the outer region. Due to this multiscale character, the classical numerical methods cease to give satisfactory numerical results and are not competitive computationally. Therefore, to overcome the shortcomings, researchers are forced to construct numerical methods that are flexible enough to provide a solution whose accuracy is independent of the perturbation parameter(s), and its singular nature can easily be captured. The sounding numerical methods on hand are

the specially designed (fitted) ones. Just to list some of these, the authors of [9–15] used the fitted operator method, the authors of [16–18] implemented the fitted mesh method, Gowrisankar and Natesan [19] constructed a layer-adapted scheme through the equidistribution of a positive integrable monitor function, and Khan et al. [20] applied variable mesh in which more mesh points are in the layer region. On the other part, the authors of [21, 22] used unfitted methods and the results yielded are not ε–uniform.

In this paper, we construct a numerical scheme for the parabolic convection-diffusion problem (1-2) through the fitted mesh method in which Crank–Nicolson discretization is used for the time variable and cubic spline in tension on layer-adapted meshes of Bakhvalov-type for the spatial variable discretization. The scheme constructed from this composition is in its first use for the problem under consideration.

2. Properties of the Continuous Problem

In this section, we consider some properties of the continuous problem through the maximum principle and bounds on the solution and on its derivatives that enable us to see a priori estimates for the solution $u(x,t)$ and its derivatives.

Lemma 1. *Let $\Pi(x,t) \in C^{2,1}(\overline{D})$. If $\Pi(x,t) \geq 0$, for all (x,t) on the boundary ∂D of the domain D, and $L_{\varepsilon,\mu}\Pi \geq 0$, for all $(x,t) \in D$, then $\Pi(x,t) \geq 0$, for all $(x,t) \in \overline{D}$.*

Proof. Assume to the contrary that there exists a point $(x^*,t^*) \in \overline{D}$ such that

$$\Pi(x^*,t^*) = \min_{(x,t)\in\overline{D}} \Pi(x,t) < 0. \tag{3}$$

It is obvious that $(x^*,t^*) \notin \partial D$ and implies $(x^*,t^*) \in D$. Applying the differential operator $L_{\varepsilon,\mu}$ in equation (1) on $\Pi(x,t)$ at the critical point (x^*,t^*) yields

$$L_{\varepsilon,\mu}\Pi(x^*,t^*) := \frac{\partial \Pi}{\partial t}(x^*,t^*) - \varepsilon \frac{\partial^2 \Pi}{\partial x^2}(x^*,t^*) - \mu a(x^*,t^*) \frac{\partial \Pi}{\partial x}(x^*,t^*) + b(x^*,t^*)\Pi(x^*,t^*). \tag{4}$$

By the partial derivative test, we have $\partial^2\Pi/\partial x^2(x^*,t^*) \geq 0$, $\partial\Pi/\partial t(x^*,t^*) = 0$, and $\partial\Pi/\partial x(x^*,t^*) = 0$. Incorporating our assumptions, $b(x^*,t^*) \geq \beta > 0$ with $\Pi(x^*,t^*) < 0$, we can arrive at $L_{\varepsilon,\mu}\Pi(x^*,t^*) \leq 0$. This contradicts the given statement. Therefore, we can conclude that the minimum of $\Pi(x,t)$ is nonnegative. □

Lemma 2. *A solution $u(x,t)$ of equation (1) satisfies the estimate*

$$\|u\| \leq \beta^{-1}\|f\| + \max|s(x)|, \tag{5}$$

where $\|.\|$ is the maximum norm.

Proof. For the proof, one can refer [23]. □

Lemma 3. *The derivatives of the solution $u(x,t)$ satisfy the following bound for all nonnegative integers i, j such that $i + 3j \leq 4$.*

$$\left\| \frac{\partial^{i+j} u}{\partial x^i \partial t^j} \right\|_{\overline{D}} \leq \begin{cases} \varepsilon^{-i/2} & \text{if } \mu^2 \leq C\varepsilon, \\ \left(\dfrac{\mu}{\varepsilon}\right)^i & \text{if } \mu^2 \geq C\varepsilon, \end{cases} \tag{6}$$

where the constant C is independent of ε and μ and depends only on the bounded derivatives of the coefficients and the source term.

Proof. The proof is given in [2]. □

3. Discretization and Mesh Generation

Consider a uniform mesh on the time domain $[0,T]$ with M mesh intervals spaced by $k = T/M$ and given by $D_t^M = \{t_m = (m-1)k, \quad m = 1, 2, \ldots, M+1\}$. Applying the Crank–Nicolson method for the time variable in equations (1) and (2), we obtain the following two-level semidiscrete scheme:

$$\begin{cases} u(x,0) = s(x), \\ L_{\varepsilon,\mu}^M \widetilde{u} \equiv -\varepsilon \widetilde{u}_{xx}(x) - \mu a(x)\widetilde{u}_x(x) + q(x)\widetilde{u}(x) = g(x), \\ \widetilde{u}(0) = 0 = \widetilde{u}(1), \end{cases} \tag{7}$$

where $q(x) = (b(x,t_m) + (2/k))$, $\widetilde{u}(x) = u(x,t_m)$, $a(x) = a(x,t_m)$, $p(x) = (b(x,t_m) - (2/k))$, $H(x) = f(x,t_m) + f(x,t_{m-1})$ and $g(x) = \varepsilon u_{xx}(x,t_{m-1}) + \mu a(x,t_{m-1})u_x(x,t_{m-1}) - p(x)u(x,t_{m-1}) + H(x)$.

A characteristic equation corresponding to equation (7) that is helpful to describe the boundary layers occurring at the two end points of $\overline{\Omega}$ is

$$-\varepsilon r^2(x) - \mu a(x) r(x) + q(x) = 0. \tag{8}$$

This defines two continuous functions

$$r_1(x) = \frac{\left(-\mu a(x) - \sqrt{(\mu a(x))^2 + 4\varepsilon q(x)}\right)}{(2\varepsilon)}, \qquad r_2(x) = \frac{\left(-\mu a(x) + \sqrt{(\mu a(x))^2 + 4\varepsilon q(x)}\right)}{(2\varepsilon)}. \tag{9}$$

Let

$$\eta_1 = -\max_{x\in\overline{\Omega}} r_1(x) \text{ and } \eta_2 = \min_{x\in\overline{\Omega}} r_2(x). \tag{10}$$

Lemma 4. *For a fixed number $0 < \rho < 1$, a certain order δ, and the solution $\widetilde{u}(x)$ of equation (3), the following holds:*

$$\left|\frac{\partial^i \tilde{u}}{\partial x^i}\right| \le C\left(1 + \eta_1^i e^{-\rho\eta_1^i x} + \eta_2^i e^{-\rho\eta_2^i (1-x)}\right), \text{ for } 0 \le i \le \delta, \quad (11)$$

where C is a constant independent of ε, μ.

Proof. For the proof, readers can refer [24]. □

Lemma 5. *The error estimate in the temporal direction satisfies*

$$\left\|\mathrm{TE}_t\right\| \le C\left(k^2\right). \quad (12)$$

Proof. The proof is given in [11]. □

3.1. Graded Mesh. Let $N+1$ be the number of graded mesh points, $0 = x_1 < x_2 < \ldots < x_{N+1} = 1$, of the interval $\overline{\Omega}$ that are arbitrarily spaced by $h_n = x_{n+1} - x_n, n = 1, \ldots, N$ yielding a space mesh $D_x^N = \{x_1, x_2, \ldots, x_{N+1}\}$. Now, divide the domain $\overline{\Omega}$ into three subintervals, namely, $[0, \tau_1]$, $[\tau_1, 1-\tau_2]$, and $[1-\tau_2, 1]$, such that the second subinterval is with equidistant $N/2$ mesh subintervals and the rest two are with gradually graded $N/4$ mesh subintervals. The two transition points τ_1 and τ_2 are chosen such that $\exp(-\eta_1 x) \le \eta_1^{-2}$ in $[\tau_1, 1]$ and $\exp(-\eta_2(1-x)) \le \eta_2^{-2}$ in $[0, 1-\tau_2]$ and given by

$$\tau_1 = \min\left\{\frac{1}{4}, \frac{2}{\eta_1}\log(\eta_1)\right\} \text{ and } \tau_2 = \min\left\{\frac{1}{4}, \frac{2}{\eta_2}\log(\eta_2)\right\}. \quad (13)$$

Since we are using nonuniform meshes in the spatial direction, we do not assume τ_1 and τ_2 to be 1/4. Furthermore, the relation $\eta_j^{-1}\log(\eta_j) \le CN^{-1}$, $j = 1, 2$ is given in [24].

For the two boundary layers, following the technique in [3], we have two generating functions

$$\begin{aligned} \psi_1(\xi) &= -\log\left(1 - 4\left(1 - 1/\eta_1\right)\xi\right) \text{ and} \\ (\xi)\psi_2 &= -\log\left(1 - 4\left(1 - 1/\eta_2\right)(1-\xi)\right), \end{aligned} \quad (14)$$

which satisfy $\psi_1(0) = 0, \psi_1(1/4) = \log(\eta_1), \psi_2(3/4) = \log(\eta_2)$, and $\psi_2(1) = 0$. Analogous to [24], the mesh points in the spatial direction can be defined by

$$x_n = \begin{cases} \dfrac{-2}{\eta_1}\log\left\{1 - \dfrac{4}{N}\left(1 - \dfrac{1}{\eta_1}\right)(n-1)\right\}, & n = 1, 2, \ldots, \dfrac{N}{4} + 1, \\ \tau_1 + 2\left(1 - \tau_1 - \tau_2\right)((n-1)/N - 1/4), & n = \dfrac{N}{4} + 2, \ldots, \dfrac{3N}{4} + 1, \\ 1 + \dfrac{2}{\eta_2}\log\left\{1 - 4\left(1 - \dfrac{1}{\eta_2}\right)\left(1 - \dfrac{(n-1)}{N}\right)\right\}, & n = \dfrac{3N}{4} + 2, \ldots, N+1. \end{cases} \quad (15)$$

This gives condensed and refined meshes in the layer regions and points where the mesh switches from fine to coarse and vice versa are chosen to be $x_{(N/4)+1} = \tau_1$ and $x_{(3N/4)+1} = 1 - \tau_2$. The step sizes are related by

$$\begin{aligned} h_1 < h_2 < \ldots h_{N/4}, \\ h_{(N/4)+1} = h_{(N/4)+2} = \ldots = h_{3N/4}, \\ h_{(3N/4)+1} > h_{(3N/4)+2} > \ldots > h_N. \end{aligned} \quad (16)$$

Lemma 6. *The mesh sizes $h_n = x_{n+1} - x_n, n = 1, 2, \ldots, N$ satisfy*

$$h_n \le \begin{cases} C\eta_1^{-1}, & n = 1, 2, \ldots, N/4, \\ CN^{-1}, & n = N/4 + 1, \ldots, 3N/4, \\ C\eta_2^{-1}, & n = 3N/4 + 1, \ldots, N. \end{cases} \quad (17)$$

Proof. For $n = 1, 2, \ldots, N/4$,

$$\begin{aligned} h_n &= x_{n+1} - x_n \\ &= \frac{-2}{\eta_1}\log\left\{1 - \frac{4}{N}\left(1 - \frac{1}{\eta_1}\right)(n)\right\} \\ &\quad - \frac{-2}{\eta_1}\log\left\{1 - \frac{4}{N}\left(1 - \frac{1}{\eta_1}\right)(n-1)\right\}, \\ &= -\frac{2}{\eta_1}\psi_1(\xi_n) + \frac{2}{\eta_1}\psi_1(\xi_{n-1}) \\ &= -\frac{2}{\eta_1}\left(\psi_1(\xi_n) - \psi_1(\xi_{n-1})\right). \end{aligned} \quad (18)$$

However, from the mean value theorem, there exists $\varsigma_n \in (\xi_{n-1}, \xi_n)$ such that

$$\psi_1'(\varsigma_n) = \left(\psi_1(\xi_n) - \psi_1(\xi_{n-1})\right)/\left(\xi_n - \xi_{n-1}\right). \quad (19)$$

This gives $h_n \le C\eta_1^{-1}, n = 1, 2, \ldots, N/4$.

For $n = N/4 + 1, \ldots, 3N/4$, from equation (15), we have $h_n = x_{n+1} - x_n = 2/N(1 - \tau_1 - \tau_2) \le CN^{-1}$. The proof in the third subinterval can be shown in a similar way as in the first subinterval. □

3.2. Total Difference Scheme. Let $Q(x, t_m)$ interpolate the solution $U(x_n, t_m) = U_n^m$ and pass through the points (x_n, t_m, U_n^m) and $(x_{n+1}, t_m, U_{n+1}^m)$ such that

$$\begin{aligned} Q(x,t_m) = {} & \frac{-h_n^2}{\theta^2 \sin(\theta)}\left[\sin\left(\frac{\theta(x-x_n)}{h_n}\right)Y_{n+1}^m + \sin\left(\frac{\theta(x_{n+1}-x)}{h_n}\right)Y_n^m\right] \\ & + \frac{h_n^2}{\theta^2}\left[\frac{x-x_n}{h_n}\left(Y_{n+1}^m + \frac{h_n^2}{\theta^2}U_{n+1}^m\right) + \frac{x_{n+1}-x}{h_n}\left(Y_n^m + \frac{\theta^2}{h_n^2}U_n^m\right)\right], \end{aligned} \tag{20}$$

where $Y_n^m = (U')_n^m$ and θ is a free parameter used to maintain consistency. The first derivatives of $Q(x, t_m)$ from the right and left of $x = x_n$ are given, respectively, by

$$\begin{aligned} Q'(x_n^+, t_m) &= \frac{U_{n+1}^m - U_n^m}{h_n} + \frac{h_n}{\theta^2}\left[(1 - \theta\csc(\theta))Y_{n+1}^m - (1 - \theta\cot(\theta))Y_n^m\right], \\ Q'(x_n^-, t_m) &= \frac{U_n^m - U_{n-1}^m}{h_{n-1}} + \frac{h_{n-1}}{\theta^2}\left[(1 - \theta\cot(\theta))Y_n^m - (1 - \theta\csc(\theta))Y_{n-1}^m\right]. \end{aligned} \tag{21}$$

Then, from the continuity condition, we have $Q'(x_n^+, t_m) = Q'(x_n^-, t_m)$ and obtain

$$\begin{aligned} & \lambda_1 h_{n-1} Y_{n-1}^m + \lambda_2 (h_{n-1} + h_n) Y_n^m + \lambda_1 h_n Y_{n+1}^m \\ & = \frac{U_{n+1}^m - U_n^m}{h_n} - \frac{U_n^m - U_{n-1}^m}{h_{n-1}}, \end{aligned} \tag{22}$$

where $\lambda_1 = (\theta\csc(\theta) - 1)/\theta^2, \lambda_2 = (1 - \theta\cot(\theta))/\theta^2$. Application of the L'Hopital's rule gives

$$\lambda_1 + \lambda_2 = 1/2. \tag{23}$$

At $x = x_{n-1}, x_n, x_{n+1}$ using the notation $W_n^m = (U')_n^m + (U')_n^{m-1}$, from equation (7), we can have

$$\begin{cases} W_{n-1}^m = \dfrac{1}{\varepsilon}\left\{-\mu\left[a_{n-1}^m (U')_{n-1}^m + a_{n-1}^{m-1}(U')_{n-1}^{m-1}\right]\right. \\ \left. + q_{n-1}^m U_{n-1}^m + p_{n-1}^{m-1} U_{n-1}^{m-1} - H_{n-1}^m\right\}, \\ W_n^m = \dfrac{1}{\varepsilon}\left\{-\mu\left[a_n^m (U')_n^m + a_n^{m-1}(U')_n^{m-1}\right] + q_n^m U_n^m\right. \\ \left. + p_n^{m-1} U_n^{m-1} - H_n^m\right\}, \\ W_{n+1}^m = \dfrac{1}{\varepsilon}\left\{-\mu\left[a_{n+1}^m (U')_{n+1}^m + a_{n+1}^{m-1}(U')_{n+1}^{m-1}\right]\right. \\ \left. + q_{n+1}^m U_{n+1}^m + p_{n+1}^{m-1} U_{n+1}^{m-1} - H_{n+1}^m\right\}, \end{cases} \tag{24}$$

where, from [25],

$$\begin{cases} (U')_{n-1}^{m} = \dfrac{1}{h_{n-1}h_n(h_{n-1}+h_n)}\left\{-\left(h_n^2+2h_{n-1}h_n\right)U_{n-1}^{m}\right. \\ \left.+(h_{n-1}+h_n)^2U_n^m-h_{n-1}^2U_{n+1}^m\right\}, \\ (U')_{n}^{m} = \dfrac{1}{h_{n-1}h_n(h_{n-1}+h_n)}\left\{-h_n^2U_{n-1}^{m}+\left(h_n^2-h_{n-1}^2\right)U_n^m\right. \\ \left.+h_{n-1}^2U_{n+1}^m\right\}, \\ (U')_{n+1}^{m} = \dfrac{1}{h_{n-1}h_n(h_{n-1}+h_n)}\left\{h_n^2U_{n-1}^{m}-(h_{n-1}\right. \\ \left.+h_n)^2U_n^m+\left(h_{n-1}^2+2h_{n-1}h_n\right)U_{n+1}^m\right\}. \end{cases} \tag{25}$$

Now, adopting the cubic spline in tension used in [25] yields

$$\lambda_1 h_{n-1}W_{n-1}^m+\lambda_2(h_{n-1}+h_n)W_n^m+\lambda_1 h_nW_{n+1}^m= \frac{U_{n+1}^m-U_n^m}{h_n}-\frac{U_n^m-U_{n-1}^m}{h_{n-1}}+\frac{U_{n+1}^{m-1}-U_n^{m-1}}{h_n}-\frac{U_n^{m-1}-U_{n-1}^{m-1}}{h_{n-1}}. \tag{26}$$

Substituting equations (24) and (25) into equation (26) and writing it in compact form, we arrive at

$$\begin{aligned} L_{\varepsilon,\mu}^{M,N}U_n^m &:= A_n^-U_{n-1}^m+A_n^0U_n^m+A_n^+U_{n+1}^m+B_n^-U_{n-1}^{m-1} \\ &\quad +B_n^0U_n^{m-1}+B_n^+U_{n+1}^{m-1} \\ &= F_n^m, \end{aligned} \tag{27}$$

where $n=2,3,\ldots,N, m=2,3,\ldots,M$,

$$\begin{aligned} A_n^- &= \mu\left[\frac{\lambda_1(h_n+2h_{n-1})}{h_{n-1}+h_n}a_{n-1}^m+\frac{\lambda_2h_n}{h_{n-1}}a_n^m-\frac{\lambda_1h_n^2}{h_{n-1}(h_{n-1}+h_n)}a_{n+1}^m\right] \\ &\quad +\lambda_1h_{n-1}q_{n-1}^m-\frac{\varepsilon}{h_{n-1}}, \\ A_n^0 &= \mu\left[\frac{-\lambda_1(h_n+h_{n-1})}{h_n}a_{n-1}^m-\frac{\lambda_2\left(h_n^2-h_{n-1}^2\right)}{h_{n-1}h_n}a_n^m+\frac{\lambda_1(h_{n-1}+h_n)}{h_{n-1}}a_{n+1}^m\right] \\ &\quad +\lambda_2(h_{n-1}+h_n)q_n^m+\frac{\varepsilon(h_n+h_{n-1})}{h_{n-1}h_n}, \\ A_n^+ &= \mu\left[\frac{\lambda_1h_{n-1}^2}{h_n(h_{n-1}+h_n)}a_{n-1}^m-\frac{\lambda_2h_{n-1}}{h_n}a_n^m-\frac{\lambda_1(h_{n-1}+2h_n)}{h_{n-1}+h_n}a_{n+1}^m\right] \\ &\quad +\lambda_1h_nq_{n+1}^m-\frac{\varepsilon}{h_n}, \\ B_n^- &= \mu\left[\frac{\lambda_1(h_n+2h_{n-1})}{h_{n-1}+h_n}a_{n-1}^{m-1}+\frac{\lambda_2h_n}{h_{n-1}}a_n^{m-1}-\frac{\lambda_1h_n^2}{h_{n-1}(h_{n-1}+h_n)}a_{n+1}^{m-1}\right] \\ &\quad +\lambda_1h_{n-1}p_{n-1}^{m-1}-\frac{\varepsilon}{h_{n-1}}, \\ B_n^0 &= \mu\left[\frac{-\lambda_1(h_n+h_{n-1})}{h_n}a_{n-1}^{m-1}-\frac{\lambda_2\left(h_n^2-h_{n-1}^2\right)}{h_{n-1}h_n}a_n^{m-1}+\frac{\lambda_1(h_{n-1}+h_n)}{h_{n-1}}a_{n+1}^{m-1}\right] \\ &\quad +\lambda_2(h_{n-1}+h_n)p_n^{m-1}+\frac{\varepsilon(h_n+h_{n-1})}{h_{n-1}h_n}, \end{aligned}$$

$$B_n^+ = \mu\left[\frac{\lambda_1 h_{n-1}^2}{h_n(h_{n-1}+h_n)}a_{n-1}^{m-1} - \frac{\lambda_2 h_{n-1}}{h_n}a_n^{m-1} - \frac{\lambda_1(h_{n-1}+2h_n)}{h_{n-1}+h_n}a_{n+1}^{m-1}\right] + \lambda_1 h_n p_{n+1}^{m-1} - \frac{\varepsilon}{h_n},$$
$$F_n^m = \lambda_1 h_{n-1}H_{n-1}^m + \lambda_2(h_n+h_{n-1})H_n^m + \lambda_1 h_n H_{n+1}^m. \tag{28}$$

The system (27) together with the given conditions is uniquely solvable. Furthermore, the matrix associated with this system of equations satisfies the property of an M-matrix that is given in [26].

4. Convergence and Stability Analysis

Obtaining stability conditions for the Crank–Nicolson by using either the Fourier analysis or the matrix method is subjected to severe restrictions. This is worse for problems with variable coefficients like in our case. Thus, the maximum principle analysis can be taken as an alternative means [27]. So, to establish the parameter uniform convergence of the proposed scheme, let us see the following lemmas.

Lemma 7. *Assume that*

$$\mu h_n + \frac{(h_n^2)}{k} \le C\varepsilon, \quad 1 \le n \le \frac{N}{4}, \tag{29a}$$

$$\frac{(h_n^2)}{k} \le C\varepsilon + \mu h_n, \quad \frac{3N}{4} + 1 \le n \le N. \tag{29b}$$

Then, under these assumptions, the matrix associated with equation (27) at each time level is an M-matrix. Hence, the operator $L_{\varepsilon,\mu}^{M,N}$ satisfies the following discrete maximum principle.

Lemma 8. *(discrete maximum principle). Let the discrete function Ψ_n^m satisfy $\Psi_1^m \ge 0$ and $\Psi_{N+1}^m \ge 0$. Then, $L_{\varepsilon,\mu}^{M,N}\Psi_n^m \ge 0$, $n = 2, \ldots, N$ implies $\Psi_n^m \ge 0, \forall n \in \{1, 2, \ldots, N+1\}$.*

Proof. To follow the proof by contradiction, let there exist a mesh point (l, m) for $l \in \{1, 2, \ldots, N+1\}$ such that

$$\Psi_l^m = \min_{1\le n\le N+1} \Psi_n^m, \tag{30}$$

and suppose $\Psi_l^m \le 0$. Then, this indicates $l \ne 1, N+1$, and for $l \in \{2, 3, \ldots, N\}$, we obtain

$$L_{\varepsilon,\mu}^{M,N}\Psi_l^m \le 0, \tag{31}$$

which contradicts the assumption $L_{\varepsilon,\mu}^{M,N}\Psi_n^m \ge 0, n = 2, \ldots, N$. This follows that $\Psi_n^m \ge 0, \forall n \in \{1, 2, \ldots, N+1\}$. □

Lemma 9. *For any discrete function Φ defined on the tensor product $\Omega_x^N \times \Omega_t^M$ such that $\Phi(x_n, t_m) = 0$ for all (x_n, t_m) on the boundary of $\Omega_x^N \times \Omega_t^M$, then*

$$\left|\Phi(x_n, t_m)\right| \le \frac{1}{q^*} \max_{1\le n\le N+1, 1\le m\le M+1} \left|L_{\varepsilon,\mu}^{N,M}\Phi(x_n, t_m)\right|, \tag{32}$$

for $q_n^m \ge q^* > 0$.

Proof. The proof follows from the application of the discrete maximum principle to a mesh function given by

$$Z^{\pm}(x_n, t_m) = \frac{1}{q^*} \max_{1\le n\le N+1, 1\le m\le M+1} \left|L_{\varepsilon,\mu}^{N,M}\Phi(x_n, t_m)\right| \pm \Phi(x_n, t_m). \tag{33}$$

□

Lemma 10. *The truncation error in the spatial direction, denoted by TE_x, satisfies*

$$\left\|\mathrm{TE}_x\right\| \le C\left(N^{-2}\right). \tag{34}$$

Proof. Let the truncation error in the spatial variable with fixed time be given by

$$\mathrm{TE}_x = A_n^- U_{n-1}^m + A_n^0 U_n^m + A_n^+ U_{n+1}^m + B_n^- U_{n-1}^{m-1} + B_n^0 U_n^{m-1} + B_n^+ U_{n+1}^{m-1} - F_n^m. \tag{35}$$

The Taylor series expansion of each term in space up to the third order derivative and collecting U_n^m, $(U')_n^m$, $(U^{'})_n^m$, $(U^{''})_n^m$, U_n^{m-1}, $(U')_n^{m-1}$, $(U^{'})_n^{m-1}$, and $(U^{''})_n^{m-1}$ give

$$\mathrm{TE}_x = \zeta_{0,n}^m U_n^m + \zeta_{1,n}^m (U')_n^m + \zeta_{2,n}^m (U'')_n^m + \zeta_{3,n}^m (U''')_n^m + \zeta_{0,n}^{m-1} U_n^{m-1} + \zeta_{1,n}^{m-1} (U')_n^{m-1} + \zeta_{2,n}^{m-1} (U''')_n^{m-1} + \zeta_{3,n}^{m-1} (U''')_n^{m-1}, \tag{36}$$

where upon simplification and restricting the expansion of the coefficients to their first term yield

$$\zeta_{0,n}^m = \zeta_{1,n}^m = \zeta_{0,n}^{m-1} = \zeta_{1,n}^{m-1} = 0,$$
$$\zeta_{2,n}^m = \zeta_{2,n}^{m-1} = \varepsilon\left(\frac{-1}{2} + \lambda_1 + \lambda_2\right)(h_{n-1} + h_n). \tag{37}$$

Table 1: Comparison of the maximum pointwise error and rate of convergence for Example 1 for $\mu = 10^{-6}$ and different values of ε.

$\varepsilon\downarrow$	$N = 32$ $M = 10$	$N = 64$ $M = 20$	$N = 128$ $M = 40$	$N = 256$ $M = 80$	$N = 512$ $M = 160$
Current method					
10^{-2}	6.2022 $e-04$	1.8723 $e-04$	9.8684 $e-05$	5.2922 $e-05$	3.0726 $e-05$
	1.7280	0.9239	0.8989	0.7844	
10^{-4}	2.2942 $e-04$	5.7523 $e-05$	1.4390 $e-05$	7.5990 $e-06$	2.7100 $e-06$
	1.9958	1.9991	0.9212	1.4875	
10^{-6}	2.2902 $e-04$	5.7428 $e-05$	1.4367 $e-05$	3.5924 $e-06$	8.9814 $e-07$
	1.9956	1.9990	1.9997	1.9999	
10^{-8}	2.2902 $e-04$	5.7427 $e-05$	1.4367 $e-05$	3.5924 $e-06$	8.9813 $e-07$
	1.9957	1.9990	1.9997	2.0000	
10^{-10}	2.2902 $e-04$	5.7427 $e-05$	1.4367 $e-05$	3.5924 $e-06$	8.9813 $e-07$
	1.9957	1.9990	1.9997	2.0000	
10^{-12}	2.2902 $e-04$	5.7427 $e-05$	1.4367 $e-05$	3.5924 $e-06$	8.9813 $e-07$
	1.9957	1.9990	1.9997	2.0000	
Method in [28]					
10^{-2}	8.6053 $e-03$	4.4951 $e-03$	2.2857 $e-03$	1.1438 $e-03$	5.7093 $e-04$
	0.937	0.976	0.999	1.002	
10^{-4}	8.6095 $e-03$	4.4529 $e-03$	2.2631 $e-03$	1.1406 $e-03$	5.7256 $e-04$
	0.951	0.976	0.988	0.994	
10^{-6}	8.6014 $e-03$	4.4513 $e-03$	2.2628 $e-03$	1.1406 $e-03$	5.7356 $e-04$
	0.951	0.976	0.988	0.994	
10^{-8}	8.6006 $e-03$	4.4512 $e-03$	2.2628 $e-03$	1.1406 $e-03$	5.7356 $e-04$
	0.951	0.976	0.988	0.994	
10^{-10}	8.6006 $e-03$	4.4512 $e-03$	2.2628 $e-03$	1.1406 $e-03$	5.7356 $e-04$
	0.951	0.976	0.988	0.994	
10^{-12}	8.6006 $e-03$	4.4512 $e-03$	2.2628 $e-03$	1.1406 $e-03$	5.7356 $e-04$
	0.951	0.976	0.988	0.994	

Table 2: Comparison of the maximum pointwise error and rate of convergence for Example 2 for $\mu = 10^{-6}$ and different values of ε.

$\varepsilon\downarrow$	$N = 32$ $M = 10$	$N = 64$ $M = 20$	$N = 128$ $M = 40$	$N = 256$ $M = 80$	$N = 512$ $M = 160$
Current method					
10^{-2}	3.7393 $e-03$	1.0548 $e-03$	2.8089 $e-04$	7.2507 $e-05$	1.8422 $e-05$
	1.8258	1.9089	1.9538	1.9767	
10^{-4}	3.9293 $e-03$	1.1111 $e-03$	2.9595 $e-04$	7.6404 $e-05$	1.9412 $e-05$
	1.8223	1.9086	1.9536	1.9767	
10^{-6}	3.9337 $e-03$	1.1117 $e-03$	2.9609 $e-04$	7.6436 $e-05$	1.9423 $e-05$
	1.8231	1.9087	1.9537	1.9765	
10^{-8}	3.9337 $e-03$	1.1117 $e-03$	2.9608 $e-04$	7.6439 $e-05$	1.9423 $e-05$
	1.8231	1.9087	1.9536	1.9765	
10^{-10}	3.9337 $e-03$	1.1117 $e-03$	2.9608 $e-04$	7.6439 $e-05$	1.9423 $e-05$
	1.8231	1.9088	1.9536	1.9765	
10^{-12}	3.9337 $e-03$	1.1117 $e-03$	2.9608 $e-04$	7.6439 $e-05$	1.9423 $e-05$
	1.8231	1.9088	1.9536	1.9765	
Method in [28]					
10^{-2}	3.6825 $e-02$	1.8188 $e-02$	8.5040 $e-03$	4.2227 $e-03$	2.1179 $e-03$
	1.018	1.097	1.010	0.995	
10^{-4}	3.9442 $e-02$	1.9359 $e-02$	9.5692 $e-03$	4.7539 $e-03$	2.3691 $e-03$
	1.027	1.016	1.009	1.005	
10^{-6}	3.9402 $e-02$	1.9391 $e-02$	9.5773 $e-03$	4.7594 $e-03$	2.3717 $e-03$
	1.023	1.018	1.009	1.005	
10^{-8}	3.9418 $e-02$	1.9392 $e-02$	9.5791 $e-03$	4.7594 $e-03$	2.3718 $e-03$
	1.023	1.017	1.009	1.005	
10^{-10}	3.9418 $e-02$	1.9392 $e-02$	9.5791 $e-03$	4.7594 $e-03$	2.3718 $e-03$
	1.023	1.017	1.009	1.005	
10^{-12}	3.9418 $e-02$	1.9392 $e-02$	9.5791 $e-03$	4.7594 $e-03$	2.3718 $e-03$
	1.023	1.017	1.009	1.005	

Table 3: Comparison of the maximum pointwise error and rate of convergence for Example 3 for $\mu = 10^{-7}$ and different values of ε.

$\varepsilon\downarrow$	$N = 64$ $M = 16$	$N = 128$ $M = 32$	$N = 256$ $M = 64$	$N = 512$ $M = 128$
Current method				
10^{-6}	2.6347 $e-05$ 1.9998	6.5876 $e-06$ 1.9996	1.6474 $e-06$ 2.0001	4.1182 $e-07$ 1.9999
10^{-7}	2.6346 $e-05$ 1.9997	6.5877 $e-06$ 1.9996	1.6474 $e-06$ 2.0001	4.1182 $e-07$ 1.9999
10^{-8}	2.6346 $e-05$ 1.9997	6.5877 $e-06$ 1.9996	1.6474 $e-06$ 2.0001	4.1182 $e-07$ 1.9999
10^{-9}	2.6346 $e-05$ 1.9997	6.5877 $e-06$ 1.9996	1.6474 $e-06$ 2.0001	4.1182 $e-07$ 1.9999
Method in [2]				
10^{-6}	3.8754 $E-5$ 1.9238	1.0214 $E-5$ 1.9646	2.6170 $E-6$ 1.9821	6.6241 $E-7$ 1.9910
10^{-7}	3.8753 $E-5$ 1.9238	3.8753 $E-5$ 1.9646	2.6170 $E-6$ 1.9821	6.6241 $E-7$ 1.9910
10^{-8}	3.8753 $E-5$ 1.9238	1.0214 $E-5$ 1.9646	2.6170 $E-6$ 1.9821	6.6241 $E-7$ 1.9910
10^{-9}	3.8753 $E-5$ 1.9238	1.0214 $E-5$ 1.9646	2.5461 $E-6$ 1.9821	6.6241 $E-7$ 1.9910

Using the relation $\eta_j^{-1}\log(\eta_j) \le \mathrm{CN}^{-1}$, $j = 1, 2$, Lemma 4 and equations (17) and (23), it can be further simplified to

$$\left\|\mathrm{TE}_x\right\| \le C\left(N^{-2}\right). \tag{38}$$

As the operator $L_{\varepsilon,\mu}^{M,N}$ satisfies the discrete maximum principle on the tensor product $D_t^M \times D_x^N$ and the error is estimated, the current method is uniformly stable in the maximum norm. Applying the triangular inequality from equations (12) and (38), we can have the following theorem. □

Theorem 1. *Let $u(x,t)$, $(x,t) \in \overline{D}$ be the solution of equations (1) and (2) and $U(x_n,t_m)$, $(x_n,t_m) \in D_x^N \times D_t^M$ be the solution of equation (13). Then, the error estimate for the fully discrete scheme is given by*

$$\max_{n,m}\left|u(x_n,t_m) - U(x_n,t_m)\right| \le C\left(N^{-2} + k^2\right). \tag{39}$$

Therefore, the presented method is convergent independent of the perturbation parameters and its rate of convergence is two.

5. Computational Results and Discussion

To verify the theoretical results experimentally, we solve the following examples.

Example 1. For the problem in [28],

$$\frac{\partial u}{\partial t} - \varepsilon\frac{\partial^2 u}{\partial x^2} - \mu(1+x)\frac{\partial u}{\partial x} + u = -16x^2(1-x)^2, \text{ subject to } u(x,0) = 0, u(0,t) = 0 = u(1,t). \tag{40}$$

Example 2. Consider the following singular perturbation initial-boundary-value problem in [28],

$$\frac{\partial u}{\partial t} - \varepsilon\frac{\partial^2 u}{\partial x^2} - \mu(1+\exp(x))\frac{\partial u}{\partial x} + \left(1+x^5\right)u = -10\exp\left(t^2\right)x^2\left(1-x^2\right), \text{subject to } u(x,0) = 0, u(0,t) = 0 = u(1,t). \tag{41}$$

Example 3. Consider the following singular perturbation initial-boundary-value problem in [2],

$$\frac{\partial u}{\partial t} - \varepsilon\frac{\partial^2 u}{\partial x^2} - \mu\left(1+x-x^2+t^2\right)\frac{\partial u}{\partial x} + (1+5xt)u = \left(x^2-x\right)\left(e^t-1\right), \text{subject to } u(x,0) = 0, u(0,t) = 0 = u(1,t). \tag{42}$$

As the considered examples have no exact solution, we calculate the absolute maximum errors using the double mesh principle as follows:

$$E_{\varepsilon,\mu}^{h,k} = \max_{1\le n\le N+1, 1\le m\le M+1}\left|U_h^k - U_{h/2}^{k/2}\right|, \tag{43}$$

where U_h^k is an approximate solution obtained using k and h step sizes in the t and x directions, respectively, and $U_{h/2}^{k/2}$ is an approximate solution obtained by bisecting the step sizes. As well, the corresponding rate of convergence is defined by

$$R = \frac{\log\left(E_{\varepsilon,\mu}^{h,k}\right) - \log\left(E_{\varepsilon,\mu}^{h/2,k/2}\right)}{\log(2)}. \tag{44}$$

The maximum absolute error and rate of convergence for Examples 1–3 are given in Tables 1–3. From these results, one can observe that the current method converges independently of the perturbation parameters and gives more accurate numerical results than the existing results available

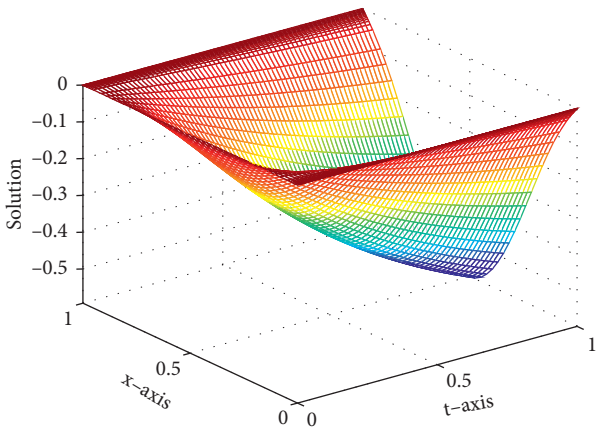

Figure 1: The numerical solution profile for Example 1 when $N = 64, M = 64, \varepsilon = 10^{-2}$, and $\mu = 10^{-10}$.

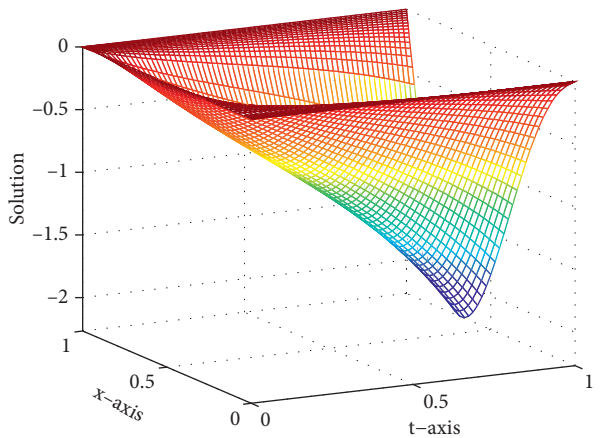

Figure 2: The numerical solution profile for Example 2 when $N = 64, M = 64, \varepsilon = 10^{-2}$, and $\mu = 10^{-10}$.

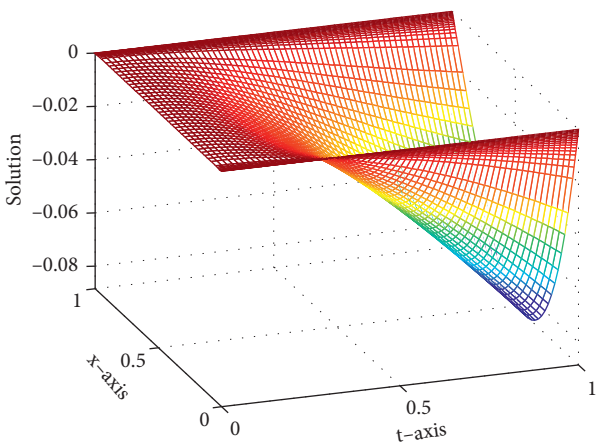

Figure 3: The numerical solution profile for Example 3 when $N = 64, M = 64, \varepsilon = 10^{-2}$, and $\mu = 10^{-10}$.

in the literature. These results are also in excellent agreement with the theoretical findings. The solution profiles illustrated in Figures 1–3 indicate the meshes in the layer regions are more condensed and refined than the outer layer. From the log-log plots in Figures 4–6, we can conclude that our method is parameter uniform.

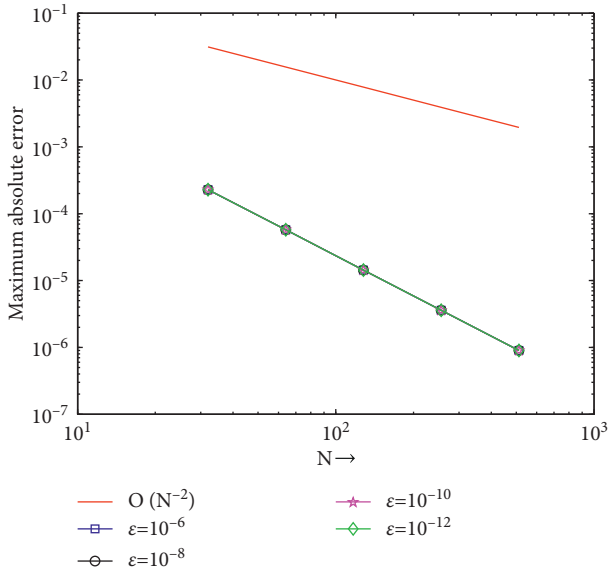

Figure 4: Log-log plot for Example 1 when $\mu = 10^{-6}$.

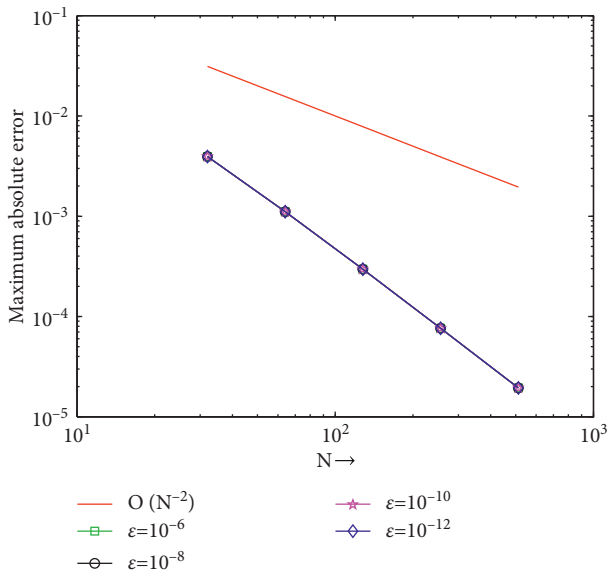

Figure 5: Log-log plot for Example 2 when $\mu = 10^{-6}$.

6. Conclusions

The present study provides the numerical solutions for a singularly perturbed unsteady-state initial-boundary-value problem with two small parameters. The method comprises of developing a scheme through discretization of the time variable by the Crank–Nicolson method on a uniform mesh and the space variable by cubic spline in tension with Bakhvalov-type mesh. The method is flexible and successful

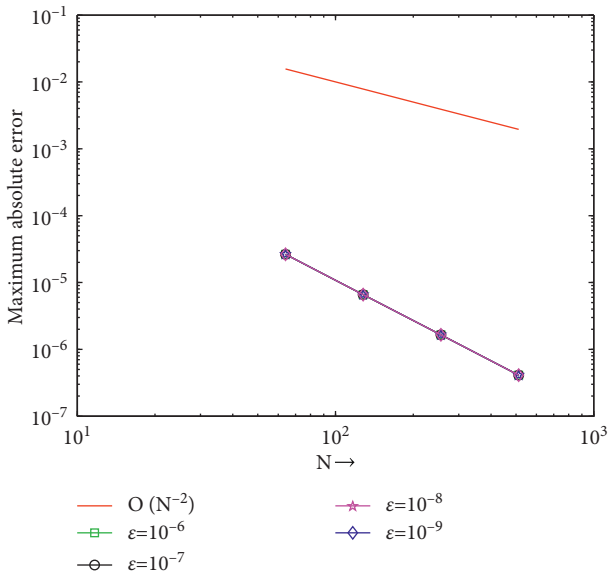

Figure 6: Log-log plot for Example 3 when $\mu = 10^{-7}$.

in capturing the sudden change of the solution behavior of the problem in the boundary layer region.

Data Availability

No data were used to support this study.

Conflicts of Interest

The authors declare that they have no conflicts of interest.

References

[1] M. Chandru, T. Prabha, P. Das, and V. Shanthi, "A numerical method for solving boundary and interior layers dominated parabolic problems with discontinuous convection coefficient and source terms," *Differential Equations and Dynamical Systems*, vol. 27, no. 1-3, pp. 91–112, 2019.

[2] V. Gupta, M. K. Kadalbajoo, and R. K. Dubey, "A parameter-uniform higher order finite difference scheme for singularly perturbed time-dependent parabolic problem with two small parameters," *International Journal of Computer Mathematics*, vol. 96, no. 3, pp. 474–499, 2019.

[3] A. Jha and M. K. Kadalbajoo, "A robust layer adapted difference method for singularly perturbed two-parameter parabolic problems," *International Journal of Computer Mathematics*, vol. 92, no. 6, pp. 1204–1221, 2015.

[4] M. Kadalbajoo and A. S. Yadaw, "Parameter-uniform finite element method for two-parameter singularly perturbed parabolic reaction-diffusion problems," *International Journal of Computational Methods*, vol. 9, no. 4, Article ID 1250047, 2012.

[5] R. E. J. O. Malley, *Introduction to singular perturbations. volume 14. Applied Mathematics and Mechanics*Academic Press, Cambridge, MA, USA, 1974.

[6] E. O'Riordan, M. Pickett, and G. Shishkin, "Parameter-uniform finite difference schemes for singularly perturbed parabolic diffusion-convection-reaction problems," *Mathematics of Computation*, vol. 75, no. 255, pp. 1135–1154, 2006.

[7] S. Pramanik, "Casson fluid flow and heat transfer past an exponentially porous stretching surface in presence of thermal radiation," *Ain Shams Engineering Journal*, vol. 5, no. 1, pp. 205–212, 2014.

[8] H. Schlichting and E. Truckenbrodt, *Aerodynamics of the Airplane*, McGraw-Hill Companies, New York NY, USA, 1979.

[9] M. K. Kadalbajoo, P. Arora, and V. Gupta, "Collocation method using artificial viscosity for solving stiff singularly perturbed turning point problem having twin boundary layers," *Computers & Mathematics with Applications*, vol. 61, no. 6, pp. 1595–1607, 2011.

[10] M. K. Kadalbajoo, P. Arora, and A. Yadaw, "Fitted collocation method for a singularly perturbed time-dependent convection-diffusion problem," *Proceedings of the Dynamic Systems and Applications*, pp. 197–204, 2012.

[11] T. B. Mekonnen and G. F. Duressa, "Computational method for singularly perturbed two-parameter parabolic convection-diffusion problems," *Cogent Mathematics & Statistics*, vol. 7, no. 1, Article ID 1829277, 2020.

[12] M. Stynes and E. O'Riordan, "Uniformly convergent difference schemes for singularly perturbed parabolic diffusion-convection problems without turning points," *Numerische Mathematik*, vol. 55, no. 5, pp. 521–544, 1989.

[13] T. Bullo, G. Duressa, and G. Degla, "Higher order fitted operator finite difference method for two-parameter parabolic convection-diffusion problems," *International Journal of Engineering and Applied Sciences*, vol. 11, no. 4, pp. 455–467, 2019.

[14] T. A. Bullo, G. A. Degla, and G. F. Duressa, "Parameter-uniform finite difference method for singularly perturbed parabolic problem with two small parameters," *International Journal for Computational Methods in Engineering Science and Mechanics*, pp. 1–9, 2021.

[15] T. A. Bullo, G. F. Duressa, and G. A. Degla, "Robust finite difference method for singularly perturbed two-parameter parabolic convection-diffusion problems," *International Journal of Computational Methods*, vol. 18, no. 2, Article ID 2050034, 2021.

[16] J. L. Gracia and E. O'Riordan, "Numerical approximations to a singularly perturbed convection-diffusion problem with a discontinuous initial condition," vol. 88, no. 4, pp. 1851–1873, 2021, https://arxiv.org/abs/2010.09305.

[17] D. Kumar, "A parameter-uniform method for singularly perturbed turning point problems exhibiting interior or twin boundary layers," *International Journal of Computer Mathematics*, vol. 96, no. 5, pp. 865–882, 2019.

[18] C. K. Mbayi, J. B. Munyakazi, and K. C. Patidar, "A robust fitted numerical method for singularly perturbed turning point problems whose solution exhibits an interior layer," *Quaestiones Mathematicae*, vol. 43, no. 1, pp. 1–24, 2020.

[19] S. Gowrisankar and S. Natesan, "An efficient robust numerical method for singularly perturbed burgers' equation," *Applied Mathematics and Computation*, vol. 346, pp. 385–394, 2019.

[20] A. Khan, I. Khan, T. Aziz, and M. Stojanovic, "A variable-mesh approximation method for singularly perturbed boundary-value problems using cubic spline in tension," *International Journal of Computer Mathematics*, vol. 81, no. 12, pp. 1513–1518, 2004.

[21] A. Khan and Shahna, "Non-polynomial quadratic spline method for solving fourth order singularly perturbed boundary value problems," *Journal of King Saud University Science*, vol. 31, no. 4, pp. 479–484, 2019.

[22] R. K. Lodhi and H. K. Mishra, "Septic b-spline method for second order self-adjoint singularly perturbed boundary-value problems," *Ain Shams Engineering Journal*, vol. 9, no. 4, pp. 2153–2161, 2018.

[23] T. B. Mekonnen and G. F. Duressa, "Uniformly convergent numerical method for two-parametric singularly perturbed parabolic convection-diffusion problems," *Journal of Applied and Computational Mechanics*, vol. 7, no. 2, pp. 535–545, 2021.

[24] M. Brdar and H. Zarin, "A singularly perturbed problem with two parameters on a bakhvalov-type mesh," *Journal of Computational and Applied Mathematics*, vol. 292, pp. 307–319, 2016.

[25] A. R. Kanth and P. M. M. Kumar, "Computational results and analysis for a class of linear and nonlinear singularly perturbed convection delay problems on shishkin mesh," *Hacettepe Journal of Mathematics and Statistics*, vol. 49, no. 1, pp. 221–235, 2020.

[26] R. B. Kellogg and A. Tsan, "Analysis of some difference approximations for a singular perturbation problem without turning points," *Mathematics of Computation*, vol. 32, no. 144, pp. 1025–1039, 1978.

[27] K. W. Morton and D. F. Mayers, *Numerical Solution of Partial Differential Equations: An Introduction*, Cambridge University Press, Cambridge, UK, 2005.

[28] M. Shivhare, P. C. Podila, and D. Kumar, "A uniformly convergent quadratic b-spline collocation method for singularly perturbed parabolic partial differential equations with two small parameters," *Journal of Mathematical Chemistry*, vol. 59, pp. 1–30, 2020.